Wavelet Based SAR Speckle Reduction and Image Compression*

J. E. Odegard, H. Guo, M. Lang, C. S. Burrus, R. O. Wells, Jr.
Computational Mathematics Laboratory
Rice University, Houston, TX-77251

L. M. Novak, M. Hiett
MIT Lincoln Laboratory
Lexington, MA-02173

June 5, 1995

Paper accepted for the Proceedings of SPIE, Algorithms for Synthetic Aperture Radar Imagery II, in SPIE Symposium on OE/Aerospace Sensing and Dual Use Photonics, 17-21 April 1995, Orlando, FL.

Abstract

This paper evaluates the performance of the recently published wavelet based algorithm for speckle reduction of SAR images. The original algorithm, based on the theory of wavelet thresholding due to Donoho and Johnstone, has been shown to improve speckle statistics. In this paper we give more extensive results based on tests performed at Lincoln Laboratory (LL). The LL benchmarks show that the SAR imagery is significantly enhanced perceptually (Figs. 3 and 4). Although the wavelet processed data results in an increase in the number of natural clutter false alarms (from trees etc.) an appropriately modified CFAR detector (i.e., by clamping the estimated clutter standard deviation (Eqn. 3)) eliminates the extra false alarms (Fig. 7). The paper also gives preliminary results on the performance of the new and improved wavelet denoising algorithm based on the shift invariant wavelet transform. By thresholding the shift invariant discrete wavelet transform we can further reduce speckle to achieve a perceptually superior SAR image with ground truth information significantly enhanced. Preliminary results on the speckle statistics of this new algorithm is improved over the classical wavelet denoising algorithm. Finally, we show that the classical denoising algorithm as proposed by Donoho and Johnstone and applied to SAR has the added benefit of achieving about 3:1 compression with essentially no loss in image fidelity.

Key words: Wavelet thresholding, denoising, SAR, speckle reduction, compression, shift invariant DWT, target detection, ATD/R.

1 Introduction

One of the major problems in processing synthetic aperture radar (SAR) images is speckle or coherent noise which typically can be modeled as multiplicative noise [10, 1]. Recently, new ideas in wavelet theory[6, 9, 7] have been applied to the problem of speckle reduction with great promise. The original wavelet based algorithm[6] applied to SAR was independently developed by Moulin [20] and Guo et al. [15, 14] The approach is to denoise (despeckle) SAR images by nonlinear thresholding of the wavelet coefficients.[6] One of the advantages is that the wavelet algorithm works on both single (polarimetric) channel SAR as well as fully polarimetric SAR. More recently a new and improved denoising algorithm has been proposed [12, 17, 16, 8, 21, 3]. Applied to SAR the new algorithm promises to be superior to the "classical wavelet denoising" algorithm.

*This research was supported in parts by ARPA, TI, BNR and the Alexander von Humboldt Foundation

While the well known polarimetric whitening filter (PWF) due to Novak [22] is based on exploiting polarimetric correlation in fully polarimetric SAR data without loss of resolution, the wavelet based algorithm for speckle reduction exploits spatial correlation with essentially no loss of image resolution. Furthermore, when combining the wavelet based method with the PWF our study shows large improvements in all relevant statistics for measuring speckle reduction [20, 14, 15, 23]. Also, while the PWF necessitates the implementation and use of a fully polarimetric SAR system, which typically is prohibitively expensive, the wavelet based algorithm offers an algorithm for reducing speckle on single channel SAR images.

Secondly considering the large amounts of data that have to be stored or quickly transmitted for military surveillance, oceanography, glaciology and agriculture studies (about 125Mb/km^2 for 1 foot resolution SAR) there is clearly a great demand for good compression algorithms. However, not much work has been devoted to studying lossy compression algorithms for sensor data and it is not clear that good image coders developed for coding optical images for human visualization are optimal for compressing various kinds of sensor data such as SAR, LADAR etc. We note however that the wavelet denoising algorithm applied to SAR [20, 14, 15, 23] inherently yields a compression of between 2:1 and 3:1. This is for the application considered in this paper achieved without loss of image fidelity. In fact the image quality is improved due to the speckle reduction. Furthermore, since the nonlinear wavelet processed SAR image is a less noisy image than the original SAR image, the resulting despeckled SAR image will be "more compressible" (there is more correlation to exploit) both with lossless as well as with lossy compression techniques. In this paper we only report on some preliminary findings with regard to the compression problem and in particular evaluate the effect of denoising on lossless compression.

2 Denoising by wavelet thresholding

In this section we will first summarize the classical results on wavelet denoising due to Donoho and Johnstone [6, 9, 7]. Secondly we will introduce the more recent results on shift invariant (or redundant/undecimated) wavelet based denoising for which details can be found in [12, 17, 16].

Let $y_i = x_i + \sigma n_i$, $i = 1, \ldots, N$ be a finite size signal of observations of the desired signal x_i that is corrupted by i.i.d. zero mean, white Gaussian noise n_i with standard deviation σ (i.e., $n_i \overset{iid}{\sim} \mathcal{N}(0,1)$). Let W and M denote the discrete wavelet transform (DWT) matrix and its inverse, respectively and denote the DWT of a signal x by X (e.g., $X = Wx$, $x = MX$). Furthermore, let $\hat{X}$ denote an estimate of X, based on the observations Y. Given some threshold function Δ we obtain an estimate of x as

$$\hat{x} = M\hat{X} = M\Delta Y = M\Delta W y. \tag{1}$$

If W is the orthogonal DWT transform matrix then Eqn. 1 describes the original wavelet denoising algorithm proposed by Donoho and Johnstone [6, 9] and we refer to this algorithm as the "classical wavelet denoising" (CWD) algorithm. In the original work by Donoho and Johnstone two thresholding schemes were considered: (i) hard thresholding (see Fig. 1c, – keep Y_i if it is above some threshold τ, set it to zero otherwise) and (ii) soft thresholding (see Fig. 1a – hard thresholding with additionally shrinkage of those values Y_i by τ that are not set to zero). In Fig. 1b and d we show two alternative thresholding functions that are optimized from a quantization-shrinkage criterion. A detailed treatment of these alternative nonlinear thresholding functions can be found in Guo et al. [13] Among several interesting properties associated with the CWD, the following are especially important: Both schemes (hard and soft thresholding) are within a logarithmic factor ($\log N$) of what is defined to be the ideal risk[6] (obtained with explicit knowledge of the noise variance). Hard thresholding typically yields a smaller mean square error (MSE) and soft thresholding achieves near minimax MSE subject to the constraint that $\hat{x}$ is (with high probability) at least as smooth as x. The CWD algorithm requires that N values have be stored and the computational complexity is $O(N)$.

In practice it was noticed that hard thresholding exhibits spurious oscillations while soft thresholding avoids those (i.e., it is a smooth estimate). Similar to classical methods (e.g., low pass filtering) there is a tradeoff in choosing the threshold (for a given threshold function) between noise reduction and oversmoothing of signal details. We do not discuss these issues here since they have been discussed at length for

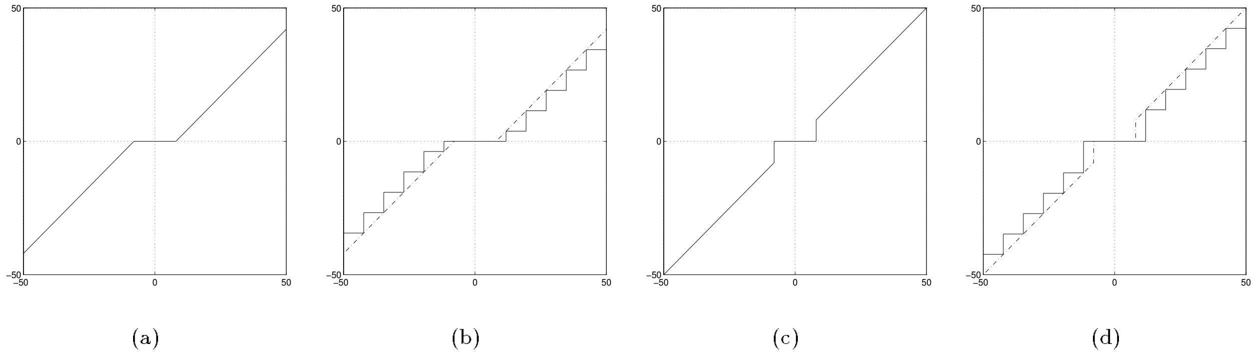

Figure 1: (a) Soft thresholding (b) Uniform Soft Shrinkage quantization (USSQ) (c) Hard thresholding (d) Uniform Hard Shrinkage Quantization (UHSQ).

the SAR problem in several previous publications.[20, 14, 15, 23] Furthermore, since the DWT is not shift invariant the CWD is not shift invariant and hence the denoising performance depends on the initial shift of the signal. A shift invariant wavelet transform can be obtained by computing the DWT of *all* shifts of the input signal (we will refer to this transform as the shift invariant DWT (SIDWT)). Since SIDWT computes a DWT for every shift the resulting transform is not orthogonal and the wavelet coefficients give a redundant representation. In fact the SIDWT requires the storage of $N \log N$ values and has computational complexity $O(N \log N)$ [18, 2, 24].

The new algorithm for denoising is based on thresholding the SIDWT and can be interpreted as averaging the result of CWD for all possible shifts of the input signal. We refer to the new algorithm as the undecimated wavelet denoising (UWD) algorithm. Detailed treatment of this algorithm can be found in [12, 17, 16, 21]. The algorithm described above was also illustrated by Donoho and Johnstone in the discussion following the presentation of "Wavelet shrinkage: Asymptopia?" [9]. The basic difference between the CWD and UWD is that the transformation matrix W for SIDWT is not square and consequently not orthogonal. However, an inverse M exists and can be computed with complexity $O(N \log N)$. In fact, the representation in the SIDWT domain contains redundancy which contributes to the improved performance (compare discussion on frames in [4]). SIDWT yields correlated noise terms, N_i, in contrast to the DWT which results in uncorrelated noise terms.

3 Despeckling of SAR

Speckle is a form of noise that can be found in several imaging systems such as SAR, sonar and laser range to mention a few. When an object is illuminated by a coherent source and the object has a surface structure that is roughly on the order of a wavelength of the incident radiation, the wave reflected from such a surface consists of contributions from many independent scattering points. Interference of these dephased but coherent waves result in the granular pattern known as *speckle*. Thus speckle tends to obscure image details and hence speckle reduction is important in most detection and recognition systems. It can be shown and simply verified by measurement that the additive white Gaussian noise (AWGN) model is a good approximation for speckle[10] when considering the SAR intensity/magnitude image (e.g., the dB image).

The goal is then to minimize the effects of speckle when the observed complex image y is a digitized SAR image. There are several algorithms for reducing speckle in SAR images [5, 22]. However, until recently [20, 14] no method existed that could significantly reduce speckle for single channel SAR images without loss of image resolution (e.g., local averaging).

The wavelet based algorithms as described in the previous section and illustrated in Fig. 2, have been studied carefully [20, 14, 15, 23] for despeckling single channel SAR as well (fully polarimetric) PWF images. In Figs. 3 and 4 we can visually observe the reduction in speckle and the corresponding perceptual

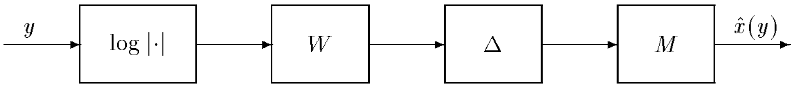

Figure 2: SAR speckle reduction via wavelet thresholding.

improvement in SAR image quality achieved by applying the two wavelet based denoising algorithms. Fig. 3a show the original PWF (1ft resolution) SAR image of the Lincoln North Building (Lincoln, MA) and the surrounding area. In Fig. 3b we show the same image processed with the CWD algorithm. Notice how perceptual quality of the SAR image is improved due to wavelet based speckle reduction. Also notice that image details are preserved (e.g., see lower left corner of the image where two almost parallel lines slightly diagonal are still separated in the processed image). In Fig. 3c we show the same image but now processed with a CWD algorithm where we replaced the standard soft thresholding operation with a uniform soft shrinkage quantizer (USSQ) (see Fig. 1b). Notice that the perceptual image quality is preserved. Finally, in Fig. 3d we show the results of applying the new wavelet based algorithm, UWD, to the original PWF image. In this image we observe further improvements of the speckle reduction over the CWD processing. Notice detail information in the image is well preserved and in several cases enhanced. Also notice how sharp edges in the image is enhanced compared to the result of CWD processing. In Figs. 4a through d we show the same for a single channel (HV) SAR image.

In Fig. 5 we show two particular regions of the SAR image which are good candidates to measure statistical speckle properties on. Fig. 5a (also referred to as Region 2) is the SAR image centered on a reflection from a car in the parking lot and hence represents a man-made object which should be at least as easy to detect in the processed image as in the unprocessed image. The second region, Fig 5b, (also referred to as Region 1) shows a part of the rooftop of the Lincoln North Building. This is a well defined surface which is known to be smooth and hence evaluation of the speckle statistics on this region should be informative. Table 1 gives the resulting speckle statistics for each of these SAR image regions. Classical measures of speckle (evaluated on any smooth region) are the standard-deviation-to-mean (std/m) ratio [10, 5] and log standard deviation (log-std) [22] which both should decrease as a result of speckle reduction. In addition we have computed target sensitive measures such as the target to clutter ratio (TC) and the deflection ratio (DR), each of which are important for a CFAR (constant false alarm rate) type detector. The deflection ratio is defined by

$$\mathrm{DR} = \frac{y - \hat{\mu}_y}{\hat{\sigma}_y} \tag{2}$$

where y is some desired target pixel, $\hat{\mu}_y$ and $\hat{\sigma}_y$ are estimate of the clutter mean and clutter standard deviation (computed in the neighborhood of the target pixel y). A two parameter CFAR detector is obtained by comparing the DR for any pixel by a threshold and conclude that a target is present if DR exceeds this threshold. Based on the evaluations performed here it is not clear what the effects of changing DR will imply in the overall performance for the CFAR detector all the time the optimal threshold will have to be adjusted according to the new statistics. It is generally believed that both the TC and DR statistics should at least not be smaller for a man-made object after speckle reduction. However, it is somewhat ambiguous to say that an increased TC or DR for a specific target implies overall improved detection performance (one also need to know how DR and TC affects "bright reflections" from natural clutter). It is in the same way hard to infer that a decreased TC or DR imply any worse detection performance. In fact we will later see that it is not necessarily true that a significantly enhanced DR statistics will result in improved performance if we assume a standard two parameter CFAR detector. We notice from Table 1 that the speckle statistics is improved for Region 1 after processing by both CWD, USSQ-CWD and UWD. Furthermore, we also notice that the new algorithm (UWD) performs better than CWD on all single channel images as well as the fully

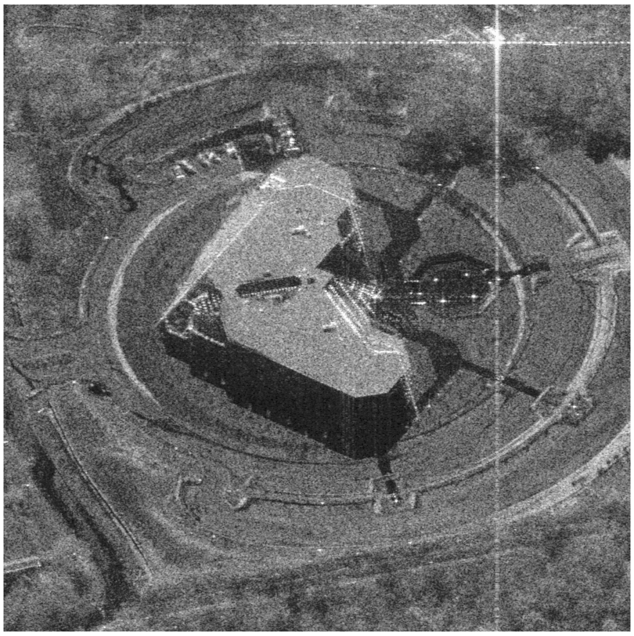

(a)

(b)

(c)

(d)

Figure 3: Fully polarimetric SAR imagery of the Lincoln North Building (Lincoln, MA) (a) Unprocessed PWF (b) Classical wavelet denoising of PWF (CWD) (c) Classical wavelet denoising of PWF with thresholding and quantization combined (USSQ-CWD) (d) shift invariant denoising of PWF (UWD).

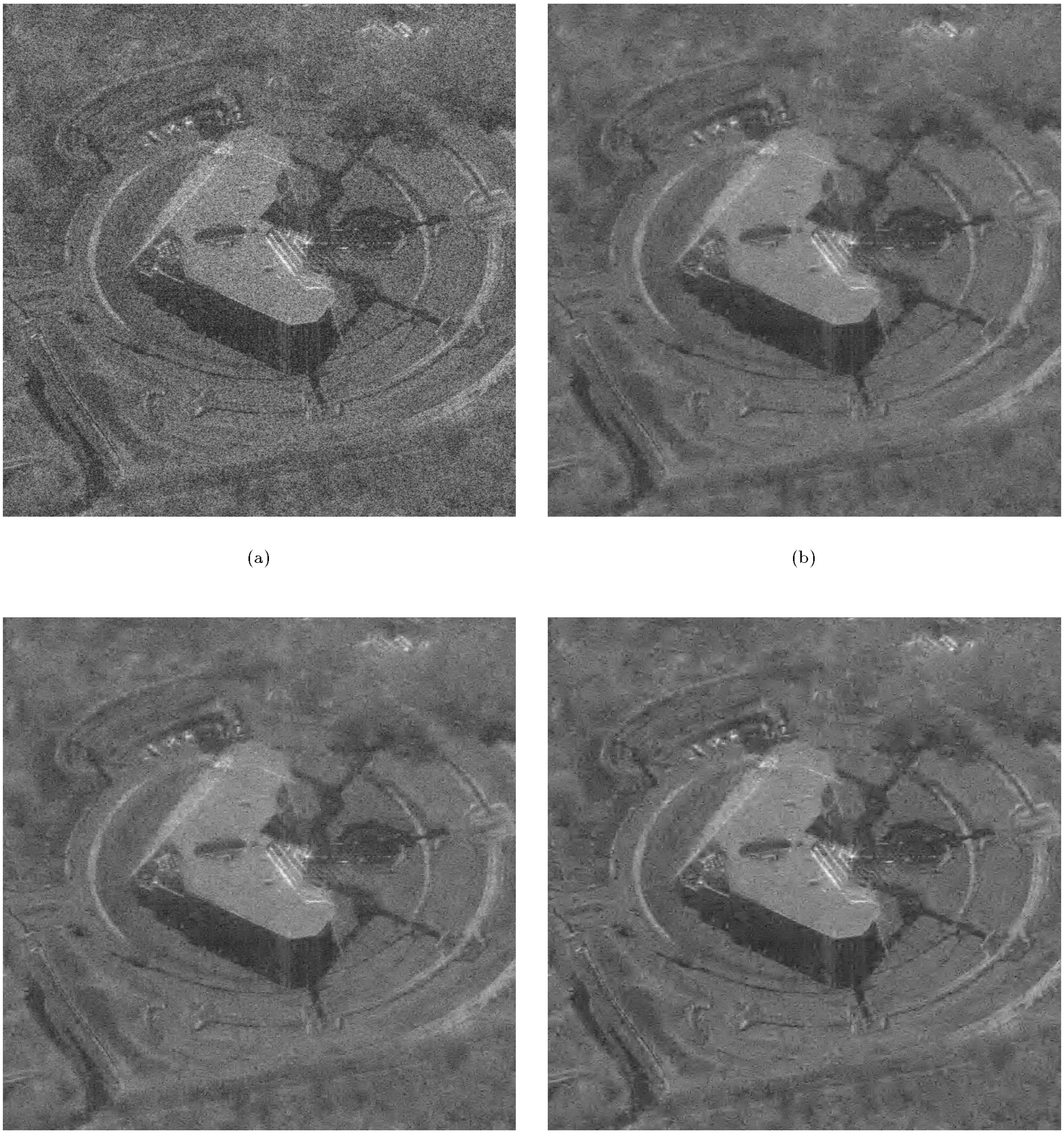

(a) (b)

(c) (d)

Figure 4: Single polarimetric channel SAR image of the Lincoln North Building (Lincoln, MA) (a) Unprocessed HV image (b) Classical wavelet denoising of HV (CWD) (c) Classical wavelet denoising of PWF with thresholding and quantization combined (USSQ-CWD) (d) shift invariant denoising of HV (UWD).

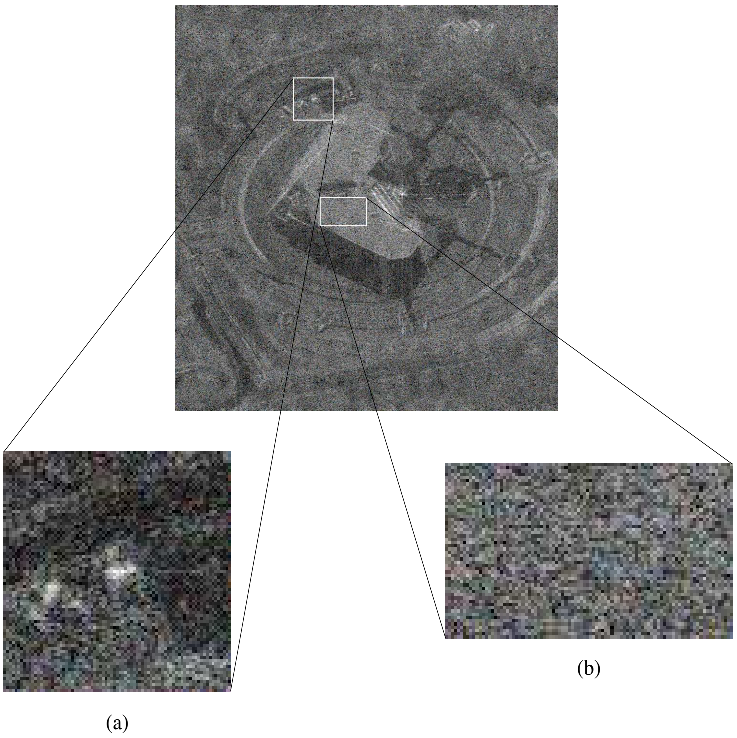

Figure 5: Illustration of two particular SAR image regions which are considered significant for the evaluation of the speckle reduction algorithm. (a) Reflection from a car in the parking lot (b) Image of a smooth region (rooftop).

Table 1: Comparison of speckle statistics for LL North building. For each polarization (1ft) we consider 4 cases: Original image (single channel or fully polarimetric), speckle reduction by Classical Wavelet Denoising (CWD), speckle reduction by CWD with uniform soft quantization (USSQ-CWD) and speckle reduction by Undecimated Wavelet Denoising (UDW).

Image Polarization		Region 1		Region 2	
		std/m	*log-std* (dB)	TC	DR
HH	Original	0.5363	5.6526	19.7927	2.8280
	CWD	0.2543	2.4787	12.7447	2.7161
	USSQ-CWD	0.2540	2.4691	12.4957	2.9253
	UWD	0.2210	2.3195	14.6217	3.4154
HV	Original	0.5415	5.6983	34.1983	4.8144
	CWD	0.2686	2.5560	27.0140	5.6690
	USSQ-CWD	0.2667	2.5416	23.8536	5.3659
	UWD	0.2401	2.3887	30.8667	6.6935
VV	Original	0.5434	5.5550	31.4152	4.7061
	CWD	0.2549	2.3709	24.2759	5.6313
	USSQ-CWD	0.2520	2.3215	20.3467	4.9549
	UWD	0.2160	2.1223	27.7310	6.7901
PWF	Original	0.3397	2.9420	30.7818	6.7347
	CWD	0.1718	1.4589	25.6036	6.7260
	USSQ-CWD	0.1519	1.3261	23.2605	6.7940
	UWD	0.1498	1.1749	30.3379	8.4508

polarimetric PWF image. In Table 2 *std/m* and *log-std* for a PWF image, CWD processed PWF image and UWD processed PWF image of four typical background clutter regions are given. Notice how the new UDW algorithm improves the performance for most areas considered. There are still some open questions of how to choose the best threshold for the UWD algorithm in the case of processing SAR images.

Table 2: Standard deviation to mean and log standard deviation for SAR image regions.

Region	*std/m*			*log-std* (dB)		
	PWF	CWD	UWD	PWF	CWD	UWD
Trees	0.5813	0.4582	0.4656	4.9404	3.9814	4.0212
Shrubs	0.3867	0.2273	0.2204	3.4292	1.9950	1.9315
Grass	0.3243	0.1611	0.1268	2.9528	1.4230	1.1218
Shadows	0.3250	0.1661	0.1401	2.8999	1.3799	1.0911

To further illustrate the potential advantages of the given algorithm consider Fig. 6. In this figure we compare the PWF image with the CWD processed PWF image in terms of maximum DR as a function about 250 SAR images of a target. For each target "look" we computed and recorded the maximum DR and we notice from Fig. 6 that the maximum DR has increased for most target looks. However, it is hard to conclude anything based this one experiment since the corresponding threshold for a CFAR type detector also will be different. Hence the detection performance based on the DR statistics might not change since the statistics of the surrounding clutter will affect the performance of the detector. With this in mind Lincoln Laboratory performed a study of the CWD algorithm on 56km^2 of SAR data. The results of this study are depicted in Table 3 and Fig. 7. In Fig. 7 we plot the probability of detection, P_d, versus false alarms per square kilometer, (FA/km^2) also known as the receiver operation characteristics (ROC) curve for the two prescreeners considered in this study (plain PWF or PWF followed by CWD). Notice that the number of natural clutter false alarms increased based on a classical two parameter CFAR detector (see

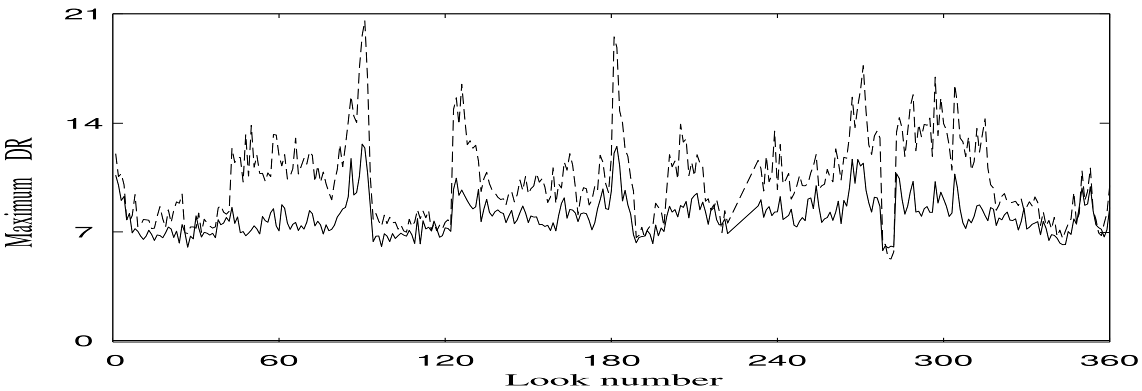

Figure 6: Maximum deflection ratio (DR) statistics as a function of target input image. The test data is obtained by collecting SAR data in spotlight mode (1 foot resolution). Dotted line: Despeckled PWF image; Solid line: PWF image.

Table 3 and Fig.7a). It was furthermore observed that most of the added natural clutter false alarms were due to small clusters of trees/shrubs surrounded by dim radar returns or located in the middle of large grassy fields and hence tend to stand out (in terms of DR statistics) from the background clutter (which is considerably smoother) after despeckling. Although the number of natural clutter false alarms increased

Table 3: Lincoln Laboratory ATD/R (automatic target detection and recognition) performance study. The test data (stripmap SAR at 1 foot resolution) was made up of a total of 4827 image chips (65 target chips, 2068 man made clutter chips and 2759 natural clutter chips). The CFAR threshold was optimized to achieve probability of detection, $P_d = 1$.

	False Alarms	
	Man made	Natural
PWF	557	70
CWD	556	251

with the application of the CWD algorithm, these additional false alarms were successfully discarded by using a clamped CFAR (Eqn. 3) detector (Fig.7b). A clamped CFAR detector is defined by computing DR as

$$\mathrm{DR} = \frac{y - \hat{\mu}_y}{\max(\hat{\sigma}_y, c)} \tag{3}$$

where c is an experimentally obtained value preventing DR from taking on large values for extremely smooth clutter neighborhoods. In Fig. 7a c was set to 0 for both the regular PWF image and the CWD processed PWF image. In Fig. 7b c was 0 for the PWF image but was experimentally chosen to be 2.5 for the CWD processed PWF image. This simple change in the CFAR detector seems to indicate that a careful study of the clutter versus target distributions of the wavelet denoised images should be performed and as a result an optimal detector could be designed.

4 Wavelet speckle reduction and SAR compression

The ability to quickly store or transmit collected survey data is of great importance for both time critical applications such as military search as well as in scientific surveys for instant refinement of wide area data collection. Furthermore, since the typical use of the collected data is for target detection, classification and

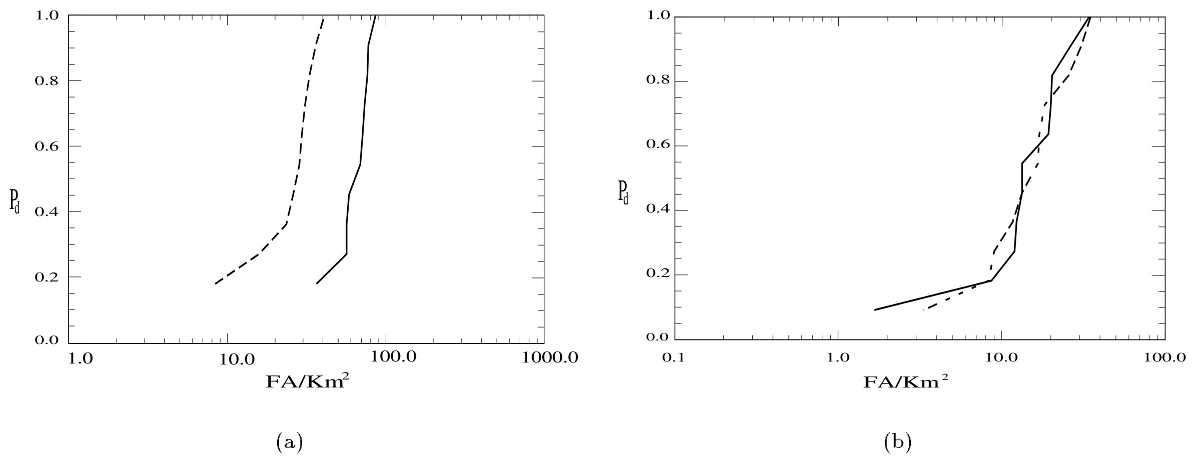

Figure 7: Receiver operation characteristic (ROC) curve for PWF image and the despeckled PWF image. Dashed line: ROC curve for PWF image. Solid line: ROC curve for CWD processed PWF image. (a) standard two parameter CFAR detector (b) two parameter CFAR detector with clamp in the standard deviation.

tracking, the requirements for an "optimal lossy" compression algorithm are typically very different from that of lossy image compression algorithms developed for compressing still images for perceptual visualization. A lot of research on still image compression has taken place over the years. However, lossy compression of sensor data such as SAR, LADAR etc. has not received much attention considering the large amount of data that is being collected and has to be stored and/or transmitted for a wide area surveillance. The main reasons for this lack of effort are mainly due to the fact that most sensor data collected is to be used by a broad range of scientists in significantly different applications. Hence, what might be defined as essentially lossless for one application might be significant data loss to another application. Due to these contradicting views lossy compression has typically been avoided and hence only lossless compression has been considered. However, realizing the explosive growth in the amount of sensor data being collected and the need to efficiently store and transmit such data in time critical applications one has come to realize that lossy compression is necessary. Some preliminary work on lossy compression of sensor data has been performed in more recent times and the two recent survey articles in the IEEE SP magazine [26, 25] signify this effort. Most of the effort has to date been focused on lossless compression techniques where one typically at best can achieve compression of about 3:1. For a more detailed treatment of lossy compression of SAR images see Werness et al.[28, 11] and Wei et al. [27].

In this section we attempt to evaluate the speckle reduction algorithm from the point of view of compression. It is clear that the thresholding operation will necessarily result in some compression, how much however is not easily answered. Our goal is to study the effect of speckle reduction on (lossless) compression. One method of evaluating the compression performance is to measure the number of zero values added to the wavelet coefficients due to the thresholding operation. However, this is not the complete story since compressibility of the despeckled image should be further improved due to the change in image noise characteristics (a smoother image). Hence here we set up the following experiment (see Fig. 8) to evaluate the total effect on "lossless" compression of a SAR images due to wavelet denoising. In Fig. 8 unless otherwise stated Q is a uniform quantizer optimized for the dynamic range of the image that is to be compressed and C is a lossless coding algorithm such Lempel-Ziv (i.e., GZIP). As seen from Fig. 8 the experiment is not truly lossless since we do require a uniform 8bit quantizer (optimized for the dynamic range of the image). However, the goal of this experiment was to measure the ability to compress the resulting uniformly quantized image with and without denoising. Hence, by lossless we only mean the encoding

$$x \longrightarrow \boxed{W} \longrightarrow \boxed{\Delta} \longrightarrow \boxed{Q} \longrightarrow \boxed{C} \longrightarrow y$$

Figure 8: Compression evaluation experiment

block used to optimally (entropy) encode the quantized image. However, it is important that the resulting decompressed SAR image maintains fidelity and that speckle statistics are preserved. We performed several compression experiments to evaluate the wavelet denoising effect on compression each of which is explained here.

1. $W = I$, $\Delta = I$ (Compress the **spatial** domain of the SAR image)
2. $W = DWT$, $\Delta = I$ (Compress the **wavelet** domain of the SAR image)
3. $W = DWT$ and
   (a) $\Delta =$ Soft thresholding (Classical wavelet denoising - **CWD**)
   (b) $\Delta =$ Uniform Shrinkage Quantizer (CWD where the soft threshold is replaced with a quantizer satisfying the shrinkage condition see Fig. 1b **USSQ-CWD**)

The compression ratios in Table 4 are given as **column:row** and the various row/columns labels indicate which algorithm (described above by bold faced words) is considered. In addition we include two row/columns the first which is the complex floating point image (which with the accuracy required can be represented by 24 bits (884 encoded[19])) and the second which is the raw SAR image (in dB) represented with 8bits accuracy. One should notice that SAR images typically are complex floating point and hence the actual compression achieved should take that in to effect. From Table 4 we see that we get compression ratios

Table 4: Compression of SAR due to wavelet based speckle reduction.

	complex	8bit	spatial	wavelet	CWT	SQ-CWD
complex	1.0					
8bit	3.0	1.0				
spatial	3.3	1.1	1.0			
wavelet	7.2	2.4	2.2	1.0		
CWD	19.8	6.6	5.9	2.0	1.0	
USSQ-CWD	23.7	7.9	6.2	3.3	1.1	1.0

of close to 7:1 without loss of image fidelity. In fact as can be seen from Table 1 the compressed image is enhanced from a speckle point of view. Also, by the numbers in column **wavelet** we see that the denoising algorithm alone (everything else kept fixed) achieves more than 2:1 compression for the image considered.

5 Summary

In this paper we have evaluated several different aspects of the wavelet despeckling algorithm. In particular we have given some new results related to the detection performance of the wavelet based despeckling algorithm in a realistic setting. The results show that applying wavelet denoising tends to cause more natural clutter false alarms. However, it was noticed that by modifying the CFAR detector the performance could be improved to equal the performance achieved without denoising. This is promising since further studies of clutter distribution versus target distribution for wavelet denoised SAR can potentially result in a new detector improving the PWF CFAR performance. We have also introduced the new undecimated wavelet denoising algorithm and showed that from a perceptual point of view as well as from observing several significant statistical speckle measures this new algorithm performs better than the classical wavelet denoising algorithm due to Donoho and Johnstone. In fact the perceptual quality of the SAR images after applying the new algorithm could improve manual observation significantly and it is hoped that this will also be true for computerized detection. Finally, we evaluated the effect of wavelet denoising on compression of SAR images and we observed that wavelet denoising alone results in a compression of close to 3:1. Combining this with optimal lossy compression methods which exploit the statistics of the resulting denoised images could result in an algorithm with significant compression with essentially no loss of information.

Acknowledgments

The authors would like to thank Donoho and others for making their work and ideas freely available over the internet. This has contributed to the speed at which new results are obtained. Our work can be found at *http://www-dsp.rice.edu*.

References

[1] H. H. Arsenault and G. April. Properties of speckle integrated with a finite aperture and logarithmically transformed. *J. Opt. Soc. Am.*, 66:1160–1163, November 1976.

[2] G. Beylkin. On the representation of operators in bases of compactly supported wavelets. *SIAM J. Numer. Anal.*, 29(6):1716–1740, 1992.

[3] R. R. Coifman. Private Communication.

[4] I. Daubechies. *Ten Lectures on Wavelets*. SIAM, Philadelphia, PA, 1992. Notes from the 1990 CBMS-NSF Conference on Wavelets and Applications at Lowell, MA.

[5] P. Dewaele, P. Wambacq, A. Oosterlinck, and J.L. Marchand. Comparison of some speckle reduction techniques for SAR images. *IGARSS*, 10:2417–2422, May 1990.

[6] D. L. Donoho. De-noising via soft-thresholding. *IEEE Trans. Inform. Theory*, to appear 1995. Also Tech. Report 409, Department of Statistics, Stanford University.

[7] D. L. Donoho and I. M. Johnstone. Ideal spatial adaptation via wavelet shrinkage. *Biometrika*, 81:425–455, 1994. Also Tech. Report 400, Department of Statistics, Stanford University, July, 1992.

[8] D. L. Donoho, I. M. Johnstone, G. Kerkyacharian, and D. Picard. Discussion of the paper wavelet shrinkage: Asymptopia? *J. R. Statist. Soc. B.*, 57(2):337–369, 1995.

[9] D. L. Donoho, I. M. Johnstone, G. Kerkyacharian, and D. Picard. Wavelet shrinkage: Asymptopia? *J. R. Statist. Soc. B.*, 57(2):301–337, 1995. Also Tech. Report 419, Department of Statistics, Stanford University, March, 1993.

[10] J. W. Goodman. Some fundamental properties of speckle. *J. Opt. Soc. Am.*, 66:1145–1150, November 1976.

[11] J. D. Gorman and S. A. Werness. Perceptual compression of magnitude-detected synthetic aperture radar imagery. In *Space and Earth Science Data Compression Workshop*, pages 93–103, NASA Conference Publication 3255, 1994. NASA.

[12] H. Guo. Redundant wavelet transform and denoising. Technical Report CML TR94-17, Rice University, Houston, TX, December 1994.

[13] H. Guo, M. Lang, J. E. Odegard, and C. S. Burrus. Nonlinear shrinkage of undecimated DWT for noise reduction and data compression. In *Proceedings of the International Conference on Digital Signal Processing*, Limassol, Cyprus, June 1995. Also Tech report CML TR95-06, Rice University, Houston, TX, March 1995.

[14] H. Guo, J. E. Odegard, M. Lang, R. A. Gopinath, I. Selesnick, and C. S. Burrus. Speckle reduction via wavelet shrinkage with application to SAR based ATD/R. In *SPIE Math. Imaging: Wavelet Applications in Signal and Image Processing*, volume 2303, pages 333–344, San Diego, CA, July 1994. Also Tech report CML TR94-03, Rice University, Houston, TX.

[15] H. Guo, J. E. Odegard, M. Lang, R. A. Gopinath, I. Selesnick, and C. S. Burrus. Wavelet based speckle reduction with application to SAR based ATD/R. In *Proc. Int. Conf. Image Processing*, volume I, pages 75–79, Austin, TX, November 1994. IEEE. Also Tech report CML TR94-02, Rice University, Houston, TX.

[16] M. Lang, H. Guo, J. E. Odegard, C. S. Burrus, and R. O. Wells Jr. Noise reduction using an undecimated discrete wavelet transform. Technical Report CML TR95-06, Rice University, CML, Houston, TX, March 1995. Submitted to IEEE SP letter.

[17] M. Lang, H. Guo, J. E. Odegard, C. S. Burrus, and R. O. Wells, Jr. Nonlinear processing of a shift-invariant DWT for noise reduction. In *SPIE conference on wavelet applications*, volume 2491, Orlando, FL, April 1995. Also Tech. report CML TR95-03, Rice University, Houston, TX.

[18] S. Mallat. Zero-crossings of a wavelet transform. *IEEE Trans. Inform. Theory*, 37(4), July 1991.

[19] T. J. Morin. Data conversion between ADT image formation processor and the VAX computer. Technical report, ECE - MS-366, Houston, TX 77251, November 1986. ADT Project Memorandum No. 47M-ADT-0053.

[20] P. Moulin. A wavelet regularization method for diffuse radar-target imaging and speckle-noise reduction. *Journal of Mathematical Imaging and Vision*, 3(1):123–134, January 1993.

[21] G. P. Nason and B. W. Silverman. Stationary wavelet transform and some statistical applications. Technical report, Department of Mathematics, University of Bristol, Bristol, U.K., February 1995. Also Tech. Report.

[22] L. M. Novak, M. C. Burl, and W. W. Irving. Optimal polarimetric processing for enhanced target detection. *IEEE Trans. AES*, 29:234–244, January 1993.

[23] J. E. Odegard. Image enhancement by nonlinear wavelet processing. In *Wavelets and Large Scale Image Processing*. International Press, October 1994. Also Tech. Report CML TR94-16, Rice University, Houston, TX.

[24] J. C. Pesquet, H. Krim, and H.Carfantan. Time invariant orthonormal wavelet representations. *Submitted to IEEE Trans. SP*, 1994.

[25] J. A. Saghri, A. G. Tescher, and J. T. Reagan. Practical transform coding of multispectral imagery. *IEEE Signal Processing Magazine*, 12(1):32–43, January 1995.

[26] V. D. Vaughn and T. S. Wilkinson. System considerations for multispectral image compression designs. *IEEE Signal Processing Magazine*, 12(1):19–31, January 1995.

[27] D. Wei, H. Guo, J. E. Odegard, M. Lang, and C. S. Burrus. Simultaneous speckle reduction and data compression using best wavelet packet bases with application to SAR based ATD/R. In *SPIE conference on wavelet applications*, volume 2491, Orlando, FL, April 1995.

[28] S. A. Werness, S. C. Wei, and R. Carpinella. Experiments with wavelets for compression of SAR data. *IEEE Trans. Geoscience and Remote Sensing*, 32(1):197–201, January 1994.